

2 Mobile Robot Kinematics

2.1 Introduction

Robot kinematics deals with the configuration of robots in their workspace, the relations between their geometric parameters, and the constraints imposed in their trajectories. The kinematic equations depend on the geometrical structure of the robot. For example, a fixed robot can have a Cartesian, cylindrical, spherical, or articulated structure, and a mobile robot may have one two, three, or more wheels with or without constraints in their motion [1–20]. The study of kinematics is a fundamental prerequisite for the study of dynamics, the stability features, and the control of the robot. The development of new and specialized robotic kinematic structures is still a topic of ongoing research, toward the end of constructing robots that can perform more sophisticated and complex tasks in industrial and societal applications [1–20].

The objectives of this chapter are as follows:

- To present the fundamental analytical concepts required for the study of mobile robot kinematics
- To present the kinematic models of nonholonomic mobile robots (unicycle, differential drive, tricycle, and car-like wheeled mobile robots (WMRs))
- To present the kinematic models of 3-wheel, 4-wheel, and multiwheel omnidirectional WMRs.

2.2 Background Concepts

As a preparation for the study of mobile robot kinematics the following background concepts are presented:

- Direct and inverse robot kinematics
- Homogeneous transformations
- Nonholonomic constraints

2.2.1 Direct and Inverse Robot Kinematics

Consider a fixed or mobile robot with generalized coordinates q_1, q_2, \dots, q_n in the joint (or actuation) space and x_1, x_2, \dots, x_m in the task space. Define the vectors:

$$\mathbf{q} = \begin{bmatrix} q_1 \\ q_2 \\ \vdots \\ q_n \end{bmatrix}, \quad \mathbf{p} = \begin{bmatrix} x_1 \\ x_2 \\ \vdots \\ x_m \end{bmatrix} \quad (2.1)$$

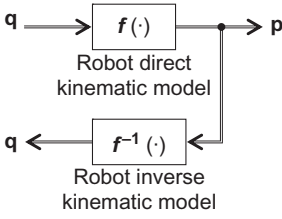


Figure 2.1 Direct and inverse robot kinematic models.

The problem of determining \mathbf{p} knowing \mathbf{q} is called the *direct kinematics* problem. In general $\mathbf{p} \in R^m$ and $\mathbf{q} \in R^n$ (R^n denotes the n -dimensional Euclidean space) are related by a nonlinear function (model) as:

$$\mathbf{p} = \mathbf{f}(\mathbf{q}), \quad \mathbf{f}(\mathbf{q}) = \begin{bmatrix} f_1(\mathbf{q}) \\ f_2(\mathbf{q}) \\ \vdots \\ f_m(\mathbf{q}) \end{bmatrix} \quad (2.2)$$

The problem of solving Eq. (2.2), that is of finding \mathbf{q} from \mathbf{p} , is called the *inverse kinematic* problem expressed by:

$$\mathbf{q} = \mathbf{f}^{-1}(\mathbf{p}) \quad (2.3)$$

The direct and inverse kinematic problems are pictorially shown in Figure 2.1.

In general, kinematics is the branch of mechanics that investigates the motion of material bodies without referring to their masses/moments of inertia and the forces/torques that produce the motion. Clearly, the kinematic equations depend on the fixed geometry of the robot in the fixed world coordinate frame.

To get these motions we must tune appropriately the motions of the joint variables, expressed by the velocities $\dot{\mathbf{q}} = [\dot{q}_1, \dot{q}_2, \dots, \dot{q}_n]^T$. We therefore need to find the differential relation of \mathbf{q} and \mathbf{p} . This is called *direct differential kinematics* and is expressed by:

$$d\mathbf{p} = \mathbf{J}d\mathbf{q} \quad (2.4)$$

where

$$d\mathbf{q} = \begin{bmatrix} dq_1 \\ \vdots \\ dq_n \end{bmatrix}, \quad d\mathbf{p} = \begin{bmatrix} dx_1 \\ \vdots \\ dx_m \end{bmatrix}$$

and the $m \times n$ matrix:

$$\mathbf{J} = \begin{bmatrix} \frac{\partial x_1}{\partial q_1} & \frac{\partial x_1}{\partial q_2} & \dots & \frac{\partial x_1}{\partial q_n} \\ \frac{\partial x_2}{\partial q_1} & \frac{\partial x_2}{\partial q_2} & \dots & \frac{\partial x_2}{\partial q_n} \\ \vdots & \vdots & \ddots & \vdots \\ \frac{\partial x_m}{\partial q_1} & \frac{\partial x_m}{\partial q_2} & \dots & \frac{\partial x_m}{\partial q_n} \end{bmatrix} = [J_{ij}] \quad (2.5)$$

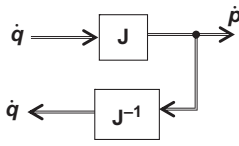


Figure 2.2 Direct and inverse differential kinematics.

with (i, j) element $J_{ij} = \partial x_i / \partial q_j$ is called the *Jacobian matrix* of the robot.¹

For each configuration q_1, q_2, \dots, q_n of the robot, the Jacobian matrix represents the relation of the displacements of the joints with the displacement of the position of the robot in the task space.

Let $\dot{\mathbf{q}} = [\dot{q}_1, \dots, \dot{q}_n]^T$ and $\dot{\mathbf{p}} = [\dot{x}_1, \dot{x}_2, \dots, \dot{x}_m]^T$ be the velocities in the joint and task spaces.

Then, dividing Eq. (2.4) by dt we get formally:

$$\frac{d\mathbf{p}}{dt} = \mathbf{J} \frac{d\mathbf{q}}{dt} \text{ or } \dot{\mathbf{p}} = \mathbf{J}\dot{\mathbf{q}} \quad (2.6)$$

Under the assumption that $m = n$ (\mathbf{J} square) and that the inverse Jacobian matrix \mathbf{J}^{-1} exists (i.e., its determinant is not zero: $\det \mathbf{J} \neq 0$), from Eq. (2.6) we get:

$$\dot{\mathbf{q}} = \mathbf{J}^{-1} \dot{\mathbf{p}} \quad (2.7)$$

This is the inverse differential kinematics equation, and is illustrated in Figure 2.2.

If $m \neq n$, then we have two cases:

Case 1 There are more equations than unknowns ($m > n$), that is, $\dot{\mathbf{q}}$ is *overspecified*. In this case \mathbf{J}^{-1} in Eq. (2.7) is replaced by the generalized inverse \mathbf{J}^\dagger given by:

$$\mathbf{J}^\dagger = (\mathbf{J}^T \mathbf{J})^{-1} \mathbf{J}^T \quad (2.8a)$$

under the condition that \mathbf{J} is full rank (i.e., $\text{rank } \mathbf{J} = \min(m, n) = n$) so as $\mathbf{J}^T \mathbf{J}$ is invertible. The expression (2.8a) of \mathbf{J}^\dagger follows by minimizing the squared norm of the difference $\dot{\mathbf{p}} - \mathbf{J}\dot{\mathbf{q}}$, that is of the function:

$$V = \|\dot{\mathbf{p}} - \mathbf{J}\dot{\mathbf{q}}\|^2 = (\dot{\mathbf{p}} - \mathbf{J}\dot{\mathbf{q}})^T (\dot{\mathbf{p}} - \mathbf{J}\dot{\mathbf{q}})$$

with respect to $\dot{\mathbf{q}}$. The optimality condition is:

$$\partial V / \partial \dot{\mathbf{q}} = -2(\dot{\mathbf{p}} - \mathbf{J}\dot{\mathbf{q}})^T \mathbf{J} = \mathbf{0}$$

¹ It is remarked that in many works the Jacobian matrix is defined as the transpose of that defined in Eq. (2.5).

which, if solved for $\dot{\mathbf{q}}$, gives:

$$\dot{\mathbf{q}} = (\mathbf{J}^T \mathbf{J})^{-1} \mathbf{J}^T \dot{\mathbf{p}} = \mathbf{J}^\dagger \dot{\mathbf{p}}$$

Case 2 There are less equations than unknowns ($m < n$), that is, $\dot{\mathbf{q}}$ is *underspecified* and many choices of $\dot{\mathbf{q}}$ lead to the same $\dot{\mathbf{p}}$. In this case we select $\dot{\mathbf{q}}$ with the minimum norm, that is, we solve the constrained minimization problem:

$$\min \|\dot{\mathbf{q}}\|^2 \text{ subject to } \dot{\mathbf{p}} - \mathbf{J}\dot{\mathbf{q}} = \mathbf{0}, \quad \dot{\mathbf{q}} \in R^n$$

Introducing the Lagrange multiplier vector λ , we get the augmented (unconstrained) Lagrangian minimization problem:

$$\min_{\dot{\mathbf{q}}, \lambda} L(\dot{\mathbf{q}}, \lambda), \quad L(\dot{\mathbf{q}}, \lambda) = \dot{\mathbf{q}}^T \dot{\mathbf{q}} + \lambda^T (\dot{\mathbf{p}} - \mathbf{J}\dot{\mathbf{q}})$$

The optimality conditions are:

$$\partial L / \partial \dot{\mathbf{q}} = 2\dot{\mathbf{q}} - \mathbf{J}^T \lambda = \mathbf{0}, \quad \partial L / \partial \lambda = \dot{\mathbf{p}} - \mathbf{J}\dot{\mathbf{q}} = \mathbf{0}$$

Solving the first for $\dot{\mathbf{q}}$ we get $\dot{\mathbf{q}} = (1/2)\mathbf{J}^T \lambda$.

Introducing this result into $\partial L / \partial \lambda = \mathbf{0}$ yields:

$$\lambda = 2(\mathbf{J}\mathbf{J}^T)^{-1} \dot{\mathbf{p}}$$

Therefore, finally we find:

$$\dot{\mathbf{q}} = \mathbf{J}^T (\mathbf{J}\mathbf{J}^T)^{-1} \dot{\mathbf{p}} = \mathbf{J}^\dagger \dot{\mathbf{p}}$$

where

$$\mathbf{J}^\dagger = \mathbf{J}^T (\mathbf{J}\mathbf{J}^T)^{-1} \tag{2.8b}$$

under the condition that $\text{rank } \mathbf{J} = m$ (i.e., $\mathbf{J}\mathbf{J}^T$ invertible). Therefore, when $m < n$ the generalized inverse [Eq. \(2.8b\)](#) should be used.

Formally, the generalized inverse \mathbf{J}^\dagger of a $m \times n$ real matrix \mathbf{J} is defined to be the unique $n \times m$ real matrix that satisfies the following four conditions:

$$\mathbf{J}\mathbf{J}^\dagger \mathbf{J} = \mathbf{J}, \quad \mathbf{J}^\dagger \mathbf{J}\mathbf{J}^\dagger = \mathbf{J}^\dagger$$

$$(\mathbf{J}\mathbf{J}^\dagger)^T = \mathbf{J}\mathbf{J}^\dagger, \quad (\mathbf{J}^\dagger \mathbf{J})^T = \mathbf{J}^\dagger \mathbf{J}$$

It follows that \mathbf{J}^\dagger has the properties:

$$(\mathbf{J}^\dagger)^\dagger = \mathbf{J}, (\mathbf{J}^T)^\dagger = (\mathbf{J}^\dagger)^T, (\mathbf{J}\mathbf{J}^T)^\dagger = (\mathbf{J}^\dagger)^T \mathbf{J}^\dagger$$

All the above relations are useful when dealing with overspecified or underspecified linear algebraic systems (encountered, e.g., in underactuated or overactuated mechanical systems).

2.2.2 Homogeneous Transformations

The position and orientation of a solid body (e.g., a robotic link) with respect to the fixed world coordinate frame $Oxyz$ (Figure 2.3) are given by a 4×4 transformation matrix \mathbf{A} , called *homogeneous transformation*, of the type:

$$\mathbf{A} = \begin{bmatrix} \mathbf{R} & \mathbf{p} \\ \mathbf{0} & 1 \end{bmatrix} \quad (2.9)$$

where \mathbf{p} is the position vector of the center of gravity O' (or some other fixed point of the link) with respect to $Oxyz$, and \mathbf{R} is a 3×3 matrix defined as:

$$\mathbf{R} = [\mathbf{n} \quad \mathbf{a} \quad \mathbf{o}] \quad (2.10)$$

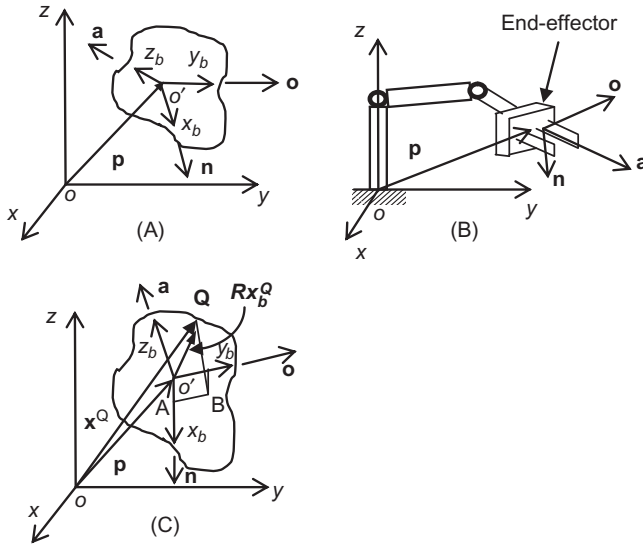


Figure 2.3 (A) Position and orientation of a solid body, (B) position and orientation of a robotic end-effector (\mathbf{a} = approach vector, \mathbf{n} = normal vector, \mathbf{o} = orientation or sliding vector), and (C) position vectors of a point Q with respect to the frames $Oxyz$ and $O'x_b y_b z_b$.

In Eq. (2.10), \mathbf{n} , \mathbf{o} and \mathbf{a} are the unit vectors along the axes x_b , y_b , z_b of the local coordinate frame $O'x_by_bz_b$. The matrix \mathbf{R} represents the rotation of $O'x_by_bz_b$ with respect to the reference (world) frame $Oxyz$. The columns \mathbf{n} , \mathbf{o} , and \mathbf{a} of \mathbf{R} are pairwise orthonormal, that is, $\mathbf{n}^T \mathbf{o} = 0$, $\mathbf{o}^T \mathbf{a} = 0$, $\mathbf{a}^T \mathbf{n} = 0$, $|\mathbf{n}| = 1$, $|\mathbf{o}| = 1$, $|\mathbf{a}| = 1$ where \mathbf{b}^T denotes the transpose (row) vector of the column vector \mathbf{b} , and $|\mathbf{b}|$ denotes the Euclidean norm of \mathbf{b} ($|\mathbf{b}| = [b_x^2 + b_y^2 + b_z^2]^{1/2}$), with b_x , b_y , and b_z being the x, y, z components of \mathbf{b} , respectively.

Thus the rotation matrix \mathbf{R} is orthonormal, that is:

$$\mathbf{R}^{-1} = \mathbf{R}^T \quad (2.11)$$

To work with homogeneous matrices we use 4-dimensional vectors (called *homogeneous vectors*) of the type:

$$\mathbf{X}^Q = \begin{bmatrix} x^Q \\ y^Q \\ z^Q \\ \dots \\ 1 \end{bmatrix} = \begin{bmatrix} \mathbf{x}^Q \\ \dots \\ 1 \end{bmatrix}, \quad \mathbf{X}_b^Q = \begin{bmatrix} x_b^Q \\ y_b^Q \\ z_b^Q \\ \dots \\ 1 \end{bmatrix} = \begin{bmatrix} \mathbf{x}_b^Q \\ \dots \\ 1 \end{bmatrix} \quad (2.12)$$

Suppose that \mathbf{X}_b^Q and \mathbf{X}^Q are the homogeneous position vectors of a point Q in the coordinate frames $O'x_by_bz_b$ and $Oxyz$, respectively. Then, from Figure 2.3C we obtain the following vectorial equation:

$$\vec{OQ} = \vec{OO'} + \vec{O'A} + \vec{AB} + \vec{BQ}$$

where

$$\vec{OQ} = \mathbf{x}^Q, \quad \vec{OO'} = \mathbf{p}, \quad \vec{O'A} = x_b^Q \mathbf{n}, \quad \vec{AB} = y_b^Q \mathbf{o}, \quad \vec{BQ} = z_b^Q \mathbf{a}.$$

Thus:

$$\mathbf{x}^Q = \mathbf{p} + x_b^Q \mathbf{n} + y_b^Q \mathbf{o} + z_b^Q \mathbf{a} = \mathbf{p} + \begin{bmatrix} \mathbf{n} & \mathbf{o} & \mathbf{a} \end{bmatrix} \begin{bmatrix} x_b^Q \\ y_b^Q \\ z_b^Q \end{bmatrix} = \mathbf{p} + \mathbf{R} \mathbf{x}_b^Q \quad (2.13a)$$

or

$$\mathbf{X}^Q = \left[\begin{array}{ccc|c} \mathbf{n} & \mathbf{o} & \mathbf{a} & \mathbf{p} \\ \hline 0 & 0 & 0 & 1 \end{array} \right] \mathbf{X}_b^Q = \mathbf{A} \mathbf{X}_b^Q \quad (2.13b)$$

where \mathbf{A} is given by Eqs. (2.9) and (2.10). Equation (2.13b) indicates that the homogeneous matrix \mathbf{A} contains both the position and orientation of the local coordinate frame $O'x_by_bz_b$ with respect to the world coordinate frame $Oxyz$.

It is easy to verify that:

$$\mathbf{A}^{-1} = \begin{bmatrix} \mathbf{R}^T & -\mathbf{R}^T \mathbf{p} \\ 0 & 1 \end{bmatrix} \quad (2.14)$$

Indeed, from Eq. (2.13a) we have: $\mathbf{x}_b^Q = -\mathbf{R}^{-1}\mathbf{p} + \mathbf{R}^{-1}\mathbf{x}^Q$, which by Eq. (2.11) gives:

$$\begin{bmatrix} \mathbf{x}_b^Q \\ 1 \end{bmatrix} = \begin{bmatrix} \mathbf{R}^T & -\mathbf{R}^T \mathbf{p} \\ 0 & 1 \end{bmatrix} \begin{bmatrix} \mathbf{x}^Q \\ 1 \end{bmatrix} = \mathbf{A}^{-1} \begin{bmatrix} \mathbf{x}^Q \\ 1 \end{bmatrix}$$

The columns \mathbf{n} , \mathbf{o} , and \mathbf{a} of \mathbf{R} consist of the direction cosines with respect to $Oxyz$. Thus the rotation matrices with respect to axes x, y, z which are represented as:

$$\mathbf{n}_x = \begin{bmatrix} 1 \\ 0 \\ 0 \end{bmatrix}, \quad \mathbf{o}_y = \begin{bmatrix} 0 \\ 1 \\ 0 \end{bmatrix}, \quad \mathbf{a}_z = \begin{bmatrix} 0 \\ 0 \\ 1 \end{bmatrix}$$

are given by:

$$\mathbf{R}_x(\phi_x) = \begin{bmatrix} 1 & 0 & 0 \\ 0 & \cos \phi_x & -\sin \phi_x \\ 0 & \sin \phi_x & \cos \phi_x \end{bmatrix} \quad (2.15a)$$

$$\mathbf{R}_y(\phi_y) = \begin{bmatrix} \cos \phi_y & 0 & -\sin \phi_y \\ 0 & 1 & 0 \\ \sin \phi_y & 0 & \cos \phi_y \end{bmatrix} \quad (2.15b)$$

$$\mathbf{R}_z(\phi_z) = \begin{bmatrix} \cos \phi_z & -\sin \phi_z & 0 \\ \sin \phi_z & \cos \phi_z & 0 \\ 0 & 0 & 1 \end{bmatrix} \quad (2.15c)$$

where ϕ_x , ϕ_y , and ϕ_z are the rotation angles with respect to x , y , and z , respectively.

In mobile robots moving on a horizontal plane, the robot is rotating only with respect to the vertical axis z , and so Eq. (2.15c) is used. Thus, for convenience, we drop the index z .

For better understanding, the upper left block of Eq. (2.15c) is obtained directly using the Oxy plane geometry shown in Figure 2.4.

Let a point $P(x_p, y_p)$ in the coordinate frame Oxy , which is rotated about the axis Oz by the angle ϕ . The coordinates of P in the frame $Ox'y'$ are x'_p and y'_p as shown in Figure 2.4. From this figure we see that:

$$\begin{aligned} x_p &= (OB) = (OD) - (BD) = x'_p \cos \phi - y'_p \sin \phi \\ y_p &= (OE) = (EZ) + (ZO) = x'_p \sin \phi + y'_p \cos \phi \end{aligned} \quad (2.16)$$

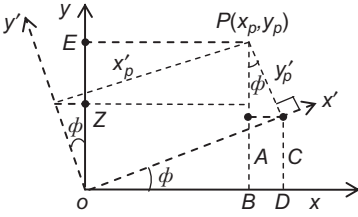


Figure 2.4 Direct trigonometric derivation of the rotation matrix with respect to axis z .

that is:

$$\begin{bmatrix} x_p \\ y_p \end{bmatrix} = \begin{bmatrix} \cos \phi & -\sin \phi \\ \sin \phi & \cos \phi \end{bmatrix} \begin{bmatrix} x'_p \\ y'_p \end{bmatrix} \quad (2.17)$$

Similarly, one can derive the respective 2×2 blocks $\mathbf{R}_x(\phi_x)$ and $\mathbf{R}_y(\phi_y)$ for the rotations about the x and y axes, respectively.

Given an open kinematic chain of n links, the homogeneous vector \mathbf{X}^n of the local coordinate frame $O_n x_n y_n z_n$ of the n th link, expressed in the world coordinate frame $Oxyz$ can be found by successive application of Eq. (2.13b), that is, as:

$$\mathbf{X}^0 = \mathbf{A}_1^0 \mathbf{A}_2^1 \cdots \mathbf{A}_n^{n-1} \mathbf{X}^n \quad (2.18)$$

where \mathbf{A}_i^{i-1} is the 4×4 homogeneous transformation matrix that leads from the coordinate frame of link i to that of link $i-1$. The matrices \mathbf{A}_i^{i-1} can be computed by the so-called *Denavit–Hartenberg* (D–H) method (Section 10.2.1). The general relation (2.18) is of the form (2.2), and provides the robot Jacobian as indicated in Eq. (2.5).

2.2.3 Nonholonomic Constraints

A nonholonomic constraint (relation) is defined to be a constraint that contains time derivatives of generalized coordinates (variables) of a system and is not integrable. To understand what this means we first define a *holonomic constraint* as any constraint which can be expressed in the form:

$$F(\mathbf{q}, t) = 0 \quad (2.19)$$

where $\mathbf{q} = [q_1, q_2, \dots, q_n]^T$ is the vector of generalized coordinates.

Now, suppose we have a constraint of the form:

$$f(\mathbf{q}, \dot{\mathbf{q}}, t) = 0 \quad (2.20)$$

If this constraint can be converted to the form:

$$F(\mathbf{q}, t) = 0 \quad (2.21)$$

we say that it is *integrable*. Therefore, although f in Eq. (2.20) contains the time derivatives $\dot{\mathbf{q}}$, it can be expressed in the holonomic form Eq. (2.21), and so it is actually a holonomic constraint. More specifically we have the following definition.

Definition 2.1 (*Nonholonomic constraint*)

A constraint of the form (2.20) is said to be *nonholonomic* if it cannot be rendered to the form (2.21) such that to involve only the generalized variables themselves.

Typical systems that are subject to nonholonomic constraints (and hence are called *nonholonomic systems*) are underactuated robots, WMRs, autonomous underwater vehicles (AUVs), and unmanned aerial vehicles (UAVs). It is emphasized that “holonomic” does not necessarily mean unconstrained. Surely, a mobile robot with no constraint is holonomic. But a mobile robot capable of only translations is also holonomic.

Nonholonomicity occurs in several ways. For example a robot has only a few motors, say $k < n$, where n is the number of degrees of freedom, or the robot has redundant degrees of freedom. The robot can produce at most k independent motions. The difference $n - k$ indicates the existence of nonholonomicity. For example, a differential drive WMR has two controls (the torques of the two wheel motors), that is, $k = 2$, and three degrees of freedom, that is, $n = 3$. Therefore, it has one ($n - k = 1$) nonholonomic constraint.

Definition 2.2 (*Pfaffian constraints*)

A nonholonomic constraint is called a Pfaffian constraint if it is linear in $\dot{\mathbf{q}}$, that is, if it can be expressed in the form:

$$\mu_i(\mathbf{q})\dot{\mathbf{q}} = 0, \quad i = 1, 2, \dots, r$$

where μ_i are linearly independent row vectors and $\mathbf{q} = [q_1, q_2, \dots, q_n]^T$.

In compact matrix form the above r Pfaffian constraints can be written as:

$$\mathbf{M}(\mathbf{q})\dot{\mathbf{q}} = \mathbf{0}, \quad \mathbf{M}(\mathbf{q}) = \begin{bmatrix} \mu_1(\mathbf{q}) \\ \mu_2(\mathbf{q}) \\ \vdots \\ \mu_r(\mathbf{q}) \end{bmatrix} \quad (2.22)$$

An example of integrable Pfaffian constraint is:

$$\mu(\mathbf{q})\dot{\mathbf{q}} = q_1\dot{q}_1 + q_2\dot{q}_2 + \dots + q_n\dot{q}_n, \quad \mathbf{q} \in R^n \quad (2.23)$$

This is integrable because it can be derived via differentiation, with respect to time, of the equation of a sphere:

$$s(\mathbf{q}) = q_1^2 + q_2^2 + \dots + q_n^2 - a^2 = 0$$

with constant radius a . The particular resulting sphere by integrating Eq. (2.23) depends on the initial state $\mathbf{q}(t)_{t=0} = \mathbf{q}_0$. The collection of all concentric spheres with center at the origin and radius “ a ” is called a *foliation* with spherical leaves. For example, if $n = 3$ the foliation produces a maximal integral manifold $(0, 0, a)$:

$$\mathcal{M} = \{\mathbf{q} \in R^3: s(\mathbf{q}) = q_1^2 + q_2^2 + q_3^2 - a^2 = 0\}$$

The nonholonomic constraint encountered in mobile robotics is the motion constraint of a disk that rolls on a plane without slipping (Figure 2.5). The no-slipping condition does not allow the generalized velocities \dot{x} , \dot{y} , and $\dot{\phi}$ to take arbitrary values.

Let r be the disk radius. Due to the no-slipping condition the generalized coordinates are constrained by the following equations:

$$\dot{x} = r\dot{\theta} \cos \phi, \quad \dot{y} = r\dot{\theta} \sin \phi \quad (2.24)$$

which are not integrable. These constraints express the condition that the velocity vector of the disk center lies in the midplane of the disk. Eliminating the velocity $v = r\dot{\theta}$ in Eq. (2.24) gives:

$$v = r\dot{\theta} = \frac{\dot{x}}{\cos \phi} = \frac{\dot{y}}{\sin \phi}$$

or

$$\dot{x} \sin \phi - \dot{y} \cos \phi = 0 \quad (2.25)$$

This is the nonholonomic constraint of the motion of the disk. Because of the kinematic constraints (2.24), the disk can attain any final configuration $(x_2, y_2, \phi_2, \theta_2)$ starting from any initial configuration $(x_1, y_1, \phi_1, \theta_1)$. This can be done in two steps as follows:

Step 1: Move the contact point (x_1, y_1) to (x_2, y_2) by rolling the disk along a line of length $(2k\pi + \theta_2 - \theta_1)r$, $k = 0, 1, 2, \dots$

Step 2: Rotate the disk about the vertical axis from ϕ_1 to ϕ_2 .

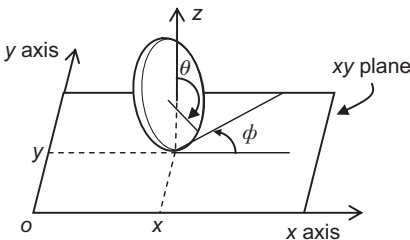


Figure 2.5 The generalized coordinates x , y , and ϕ .

Given a kinematic constraint one has to determine whether it is integrable or not. This can be done via the *Frobenius theorem* which uses the differential geometry concepts of *distributions* and *Lie Brackets*. We will come to this later (Section 6.2.1).

Two other systems that are subject to nonholonomic constraints are the *rolling ball* on a plane without spinning on place, and the *flying airplane* that cannot instantaneously stop in the air or move backward.

2.3 Nonholonomic Mobile Robots

The kinematic models of the following nonholonomic WMRs will be derived:

- Unicycle
- Differential drive WMR
- Tricycle WMR
- Car-like WMR

2.3.1 Unicycle

Unicycle has a kinematic model which is used as a basis for many types of nonholonomic WMRs. For this reason this model has attracted much theoretical attention by WMR controlists and nonlinear systems workers.

Unicycle is a conventional wheel rolling on a horizontal plane, while keeping its body vertical (Figure 2.5). The unicycle configuration (as seen from the bottom via a glass floor) is shown in Figure 2.6.

Its configuration is described by a vector of generalized coordinates: $\mathbf{p} = [x_Q, y_Q, \phi]^T$, that is, the position coordinates of the point of contact Q with the ground in the fixed coordinate frame Oxy , and its orientation angle ϕ with respect to the x axis. The linear velocity of the wheel is v_Q and its angular velocity about its instantaneous rotational axis is $v_\phi = \dot{\phi}$. From Figure 2.6, we find:

$$\dot{x}_Q = v_Q \cos \phi, \quad \dot{y}_Q = v_Q \sin \phi, \quad \dot{\phi} = v_\phi \quad (2.26)$$

Eliminating v_Q from the first two equations (2.26) we find the nonholonomic constraint (2.25):

$$-\dot{x}_Q \sin \phi + \dot{y}_Q \cos \phi = 0 \quad (2.27)$$

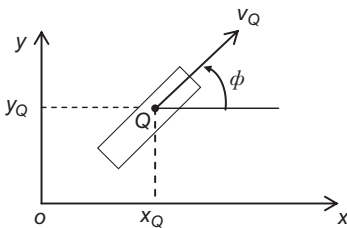


Figure 2.6 Kinematic structure of a unicycle.

Using the notation $v_1 = v_Q$ and $v_2 = v_\phi$, for simplicity, the kinematic model (2.26) of the unicycle can be written as:

$$\dot{\mathbf{p}} = \begin{bmatrix} \cos \phi \\ \sin \phi \\ 0 \end{bmatrix} v_1 + \begin{bmatrix} 0 \\ 0 \\ 1 \end{bmatrix} v_2, \quad \dot{\mathbf{p}} = \begin{bmatrix} \dot{x}_Q \\ \dot{y}_Q \\ \dot{\phi} \end{bmatrix} \quad (2.28a)$$

or

$$\dot{\mathbf{p}} = \mathbf{J}\dot{\mathbf{q}}, \quad \dot{\mathbf{q}} = [v_1, v_2]^T \quad (2.28b)$$

where \mathbf{J} is the system Jacobian matrix:

$$\mathbf{J} = \begin{bmatrix} \cos \phi & 0 \\ \sin \phi & 0 \\ 0 & 1 \end{bmatrix} \quad (2.28c)$$

The linear velocity $v_1 = v_Q$ and the angular velocity $v_\phi = v_2$ are assumed to be the action (joint) variables of the system.

The model (2.28a) belongs to the special class of nonlinear systems, called *affine systems*, and described by a dynamic equation of the form (Chapter 6):

$$\dot{\mathbf{x}} = \mathbf{g}_0(\mathbf{x}) + \sum_{i=1}^m \mathbf{g}_i(\mathbf{x}) u_i \quad (2.29a)$$

$$= \mathbf{g}_0(\mathbf{x}) + \mathbf{G}(\mathbf{x})\mathbf{u} \quad (2.29b)$$

where $u_i (i = 1, 2, \dots, m)$ appear linearly, and:

$$\mathbf{x} = [x_1, x_2, \dots, x_n]^T \in \mathcal{X}, \quad \mathbf{u} = [u_1, u_2, \dots, u_m]^T \in \mathcal{U} \quad (2.30)$$

$$\mathbf{G}(\mathbf{x}) = [\mathbf{g}_1(\mathbf{x}) : \mathbf{g}_2(\mathbf{x}) : \dots : \mathbf{g}_m(\mathbf{x})]$$

If $m < n$ the system has a less number of actuation variables (controls) than the degrees of freedom under control and is known as *underactuated* system. If $m > n$ we have an *overactuated* system. In practice, usually $m < n$. The vector \mathbf{x} is actually the state vector of the system and \mathbf{u} the control vector. The term $\mathbf{g}_0(\mathbf{x})$ is called “drift,” and the system with $\mathbf{g}_0(\mathbf{x}) = \mathbf{0}$ is called a “driftless” system. The column vector set:

$$\mathbf{g}_1(\mathbf{x}) = \begin{bmatrix} g_{11}(\mathbf{x}) \\ g_{12}(\mathbf{x}) \\ \vdots \\ g_{1n}(\mathbf{x}) \end{bmatrix}, \quad \mathbf{g}_2(\mathbf{x}) = \begin{bmatrix} g_{21}(\mathbf{x}) \\ g_{22}(\mathbf{x}) \\ \vdots \\ g_{2n}(\mathbf{x}) \end{bmatrix}, \dots, \quad \mathbf{g}_m(\mathbf{x}) = \begin{bmatrix} g_{m1}(\mathbf{x}) \\ g_{m2}(\mathbf{x}) \\ \vdots \\ g_{mn}(\mathbf{x}) \end{bmatrix} \quad (2.31)$$

is referred to as the system's *vector field*. It is assumed that the set \mathcal{U} contains at least an open set that involves the origin of R^m . If \mathcal{U} does not contain the origin, then the system is not “driftless.”

The unicycle model (2.28a) is a 2-input driftless affine system with two vector fields:

$$\mathbf{g}_1 = \begin{bmatrix} \cos \phi \\ \sin \phi \\ 0 \end{bmatrix}, \quad \mathbf{g}_2 = \begin{bmatrix} 0 \\ 0 \\ 1 \end{bmatrix} \quad (2.32)$$

The Jacobian formulation (2.28c) organizes the two column vector fields into a matrix $\mathbf{J} = \mathbf{G}$. Each action variable $u_i \in R$ in Eq. (2.29a) is actually a coefficient that determines how much of $\mathbf{g}_i(\mathbf{x})$ is contributing into the result $\dot{\mathbf{x}}$. The vector field $\mathbf{g}_1(\phi)$ of the unicycle allows *pure translation*, and the field \mathbf{g}_2 allows *pure rotation*.

2.3.2 Differential Drive WMR

Indoor and other mobile robots use the differential drive locomotion type (Figure 1.20). The *Pioneer* WMR shown in Figure 1.11 is an example of differential drive WMR. The geometry and kinematic parameters of this robot are shown in Figure 2.7. The pose (position/orientation) vector of the WMR and its speed are respectively:

$$\mathbf{p} = \begin{bmatrix} x_Q \\ y_Q \\ \phi \end{bmatrix}, \quad \dot{\mathbf{p}} = \begin{bmatrix} \dot{x}_Q \\ \dot{y}_Q \\ \dot{\phi} \end{bmatrix} \quad (2.33)$$

The angular positions and speeds of the left and right wheels are $\{\theta_l, \dot{\theta}_l\}, \{\theta_r, \dot{\theta}_r\}$, respectively.

The following assumptions are made:

- Wheels are rolling without slippage
- The guidance (steering) axis is perpendicular to the plane Oxy
- The point Q coincides with the center of gravity G , that is, $\|\vec{GQ}\| = 0$.²

Let v_l and v_r be the linear velocity of the left and right wheel respectively, and v_Q the velocity of the wheel midpoint Q of the WMR. Then, from Figure 2.7A we get:

$$v_r = v_Q + a\dot{\phi}, \quad v_l = v_Q - a\dot{\phi} \quad (2.34a)$$

Adding and subtracting v_r and v_l we get

$$v_Q = \frac{1}{2}(v_r + v_l), \quad 2a\dot{\phi} = v_r - v_l \quad (2.34b)$$

² In Figure 2.7, the points Q and G are shown distinct in order to use the same figure in all configurations with Q and G separated by distance b .

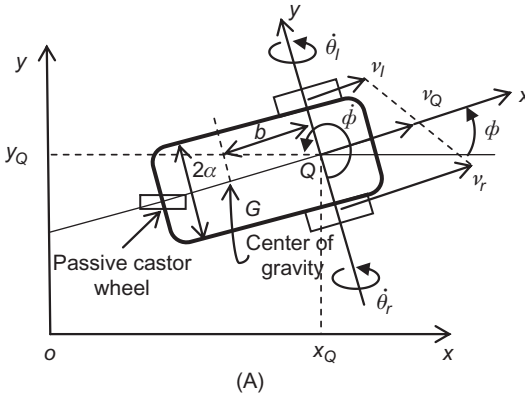
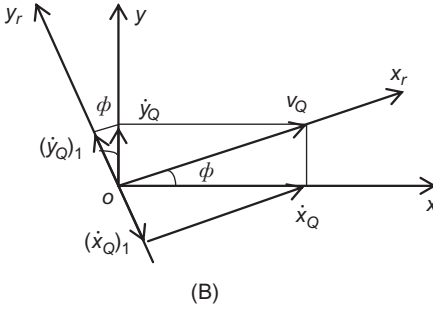


Figure 2.7 (A) Geometry of differential drive WMR, (B) Diagram illustrating the nonholonomic constraint.



where, due to the nonslippage assumption, we have $v_r = r\dot{\theta}_r$ and $v_l = r\dot{\theta}_l$. As in the unicycle case \dot{x}_Q and \dot{y}_Q are given by:

$$\dot{x}_Q = v_Q \cos \phi, \quad \dot{y}_Q = v_Q \sin \phi \quad (2.35)$$

and so the kinematic model of this WMR is described by the following relations:

$$\dot{x}_Q = \frac{r}{2}(\dot{\theta}_r \cos \phi + \dot{\theta}_l \cos \phi) \quad (2.36a)$$

$$\dot{y}_Q = \frac{r}{2}(\dot{\theta}_r \sin \phi + \dot{\theta}_l \sin \phi) \quad (2.36b)$$

$$\dot{\phi} = \frac{r}{2a}(\dot{\theta}_r - \dot{\theta}_l) \quad (2.36c)$$

Analogously to Eq. (2.28a,b) the kinematic model (2.36a–c) can be written in the *driftless affine* form:

$$\dot{\mathbf{p}} = \begin{bmatrix} (r/2)\cos \phi \\ (r/2)\sin \phi \\ r/2a \end{bmatrix} \dot{\theta}_r + \begin{bmatrix} (r/2)\cos \phi \\ (r/2)\sin \phi \\ -r/2a \end{bmatrix} \dot{\theta}_l \quad (2.37a)$$

or

$$\dot{\mathbf{p}} = \mathbf{J}\dot{\mathbf{q}} \quad (2.37b)$$

where

$$\dot{\mathbf{p}} = \begin{bmatrix} \dot{x}_Q \\ \dot{y}_Q \\ \dot{\phi} \end{bmatrix}, \quad \dot{\mathbf{q}} = \begin{bmatrix} \dot{\theta}_r \\ \dot{\theta}_l \end{bmatrix} \quad (2.37c)$$

and \mathbf{J} is the WMR's Jacobian:

$$\mathbf{J} = \begin{bmatrix} (r/2)\cos \phi & (r/2)\cos \phi \\ (r/2)\sin \phi & (r/2)\sin \phi \\ r/2a & -r/2a \end{bmatrix} \quad (2.37d)$$

Here, the two 3-dimensional vector fields are:

$$\mathbf{g}_1 = \begin{bmatrix} (r/2)\cos \phi \\ (r/2)\sin \phi \\ r/2a \end{bmatrix}, \quad \mathbf{g}_2 = \begin{bmatrix} (r/2)\cos \phi \\ (r/2)\sin \phi \\ -r/2a \end{bmatrix} \quad (2.38)$$

The field \mathbf{g}_1 allows the rotation of the right wheel, and \mathbf{g}_2 allows the rotation of the left wheel. Eliminating v_Q in Eq. (2.35) we get as usual the nonholonomic constraint (2.25) or (2.27).

$$-\dot{x}_Q \sin \phi + \dot{y}_Q \cos \phi = 0 \quad (2.39)$$

which expresses the fact that the point Q is moving along Qx_r , and its velocity along the axis Qy_r is zero (no lateral motion), that is (Figure 2.7B):

$$-(\dot{x}_Q)_1 + (\dot{y}_Q)_1 = 0$$

where $(\dot{x}_Q)_1 = \dot{x}_Q \sin \phi$ and $(\dot{y}_Q)_1 = \dot{y}_Q \cos \phi$.

The Jacobian matrix \mathbf{J} in Eq. (2.37d) has three rows and two columns, and so it is not invertible. Therefore, the solution of Eq. (2.37b) for $\dot{\mathbf{q}}$ is given by:

$$\dot{\mathbf{q}} = \mathbf{J}^\dagger \dot{\mathbf{p}} \quad (2.40)$$

where \mathbf{J}^\dagger is the generalized inverse of \mathbf{J} given by Eq. (2.8a). However, here \mathbf{J}^\dagger can be computed directly by using Eq. (2.34a), and observing from Figure 2.7B that:

$$v_Q = \dot{x}_Q \cos \phi + \dot{y}_Q \sin \phi$$

Thus, using this equation in Eq. (2.34a) we obtain:

$$\begin{aligned} r\dot{\theta}_r &= \dot{x}_Q \cos \phi + \dot{y}_Q \sin \phi + a\dot{\phi} \\ r\dot{\theta}_l &= \dot{x}_Q \cos \phi + \dot{y}_Q \sin \phi - a\dot{\phi} \end{aligned} \quad (2.41a)$$

that is:

$$\begin{bmatrix} \dot{\theta}_r \\ \dot{\theta}_l \end{bmatrix} = \frac{1}{r} \begin{bmatrix} \cos \phi & \sin \phi & a \\ \cos \phi & \sin \phi & -a \end{bmatrix} \begin{bmatrix} \dot{x}_Q \\ \dot{y}_Q \\ \dot{\phi} \end{bmatrix}$$

or

$$\dot{\mathbf{q}} = \mathbf{J}^\dagger \dot{\mathbf{p}} \quad (2.41b)$$

where³ :

$$\mathbf{J}^\dagger = \frac{1}{r} \begin{bmatrix} \cos \phi & \sin \phi & a \\ \cos \phi & \sin \phi & -a \end{bmatrix} \quad (2.41c)$$

The nonholonomic constraint (2.39) can be written as:

$$\mathbf{M}\dot{\mathbf{p}} = 0, \quad \mathbf{M} = \begin{bmatrix} -\sin \phi & \cos \phi & 0 \end{bmatrix} \quad (2.42)$$

Clearly, if $\dot{\theta}_r \neq \dot{\theta}_l$, then the difference between $\dot{\theta}_r$ and $\dot{\theta}_l$ determines the robot's rotation speed $\dot{\phi}$ and its direction. The instantaneous curvature radius R is given by (Eq. 1.1):

$$R = \frac{v_Q}{\dot{\phi}} = a \left(\frac{v_r + v_l}{v_r - v_l} \right), \quad v_r \geq v_l \quad (2.43a)$$

and the instantaneous curvature coefficient is:

$$\kappa = 1/R \quad (2.43b)$$

Example 2.1

Derive the kinematic relations (2.35) using the rotation matrix concept (2.17).

Solution

Here, the point $P(x_p, y_p)$ of Figure 2.4 is the point $Q(x_Q, y_Q)$ in Figure 2.7. The WMR velocities along the local coordinate axes Qx_r and Qy_r are \dot{x}_r and \dot{y}_r . The corresponding velocities in the world coordinate frame are \dot{x}_Q and \dot{y}_Q . Therefore, for a given ϕ , (2.17) gives:

$$\begin{bmatrix} \dot{x}_Q \\ \dot{y}_Q \end{bmatrix} = \begin{bmatrix} \cos \phi & -\sin \phi \\ \sin \phi & \cos \phi \end{bmatrix} \begin{bmatrix} \dot{x}_r \\ \dot{y}_r \end{bmatrix} \quad (2.44)$$

³ As an exercise, the reader is advised to derive Eq. (2.41c) using Eq. (2.8a).

Now, the condition of no lateral wheel movement implies that

$$\dot{y}_r = 0 \begin{bmatrix} \cos \phi & -\sin \phi \\ \sin \phi & \cos \phi \end{bmatrix}$$

and $\dot{x}_r = v_Q$. Therefore, the above relation gives:

$$\dot{x}_Q = v_Q \cos \phi \text{ and } \dot{y}_Q = v_Q \sin \phi$$

as desired.

Example 2.2

Derive the kinematic equations and constraints of a differential drive WMR by relaxing the no-slipping condition of the wheels' motion.

Solution

We will work with the WMR of [Figure 2.7](#). Considering the rotation about the center of gravity G we get the following relations:

$$\dot{x}_G = \dot{x}_Q + b\dot{\phi} \sin \phi$$

$$\dot{y}_G = \dot{y}_Q - b\dot{\phi} \cos \phi$$

Therefore, the kinematic equations [\(2.41a\)](#) and the nonholonomic constraint [\(2.42\)](#) become:

$$r\dot{\theta}_r = \dot{x}_G \cos \phi + \dot{y}_G \sin \phi + a\dot{\phi}$$

$$r\dot{\theta}_l = \dot{x}_G \cos \phi + \dot{y}_G \sin \phi - a\dot{\phi}$$

$$-\dot{x}_G \sin \phi + \dot{y}_G \cos \phi + b\dot{\phi} = 0$$

Now, assume that the wheels are subject to longitudinal and lateral slip [\[10\]](#). To include the slip into the kinematics of the robot, we introduce two variables w_r, w_l for the longitudinal slip displacements of the right wheel and left wheel, respectively, and two variables z_r, z_l for the corresponding lateral slip displacements. Thus, here:

$$\mathbf{p} = [x_G, y_G, \phi, w_r, w_l, z_r, z_l]^T$$

The slipping wheels' velocities are now given by:

$$v_r = (r\dot{\theta}_r - \dot{w}_r) \cos \zeta_r, \quad v_l = (r\dot{\theta}_l - \dot{w}_l) \cos \zeta_l$$

where ζ_r and ζ_l are the steering angles of the wheels.

Using these relations for v_r and v_l the above kinematic equations are written as:

$$v_r = (r\dot{\theta}_r - \dot{w}_r)\cos \zeta_r = \dot{x}_G \cos \phi + \dot{y}_G \sin \phi + a\dot{\phi}$$

$$v_l = (r\dot{\theta}_l - \dot{w}_l)\cos \zeta_l = \dot{x}_G \cos \phi + \dot{y}_G \sin \phi - a\dot{\phi}$$

and the nonholonomic constraint becomes:

$$-\dot{x}_G \sin \phi + \dot{y}_G \cos \phi + b\dot{\phi} - \dot{z}_r \cos \zeta_r = 0$$

$$-\dot{x}_G \sin \phi + \dot{y}_G \cos \phi + b\dot{\phi} - \dot{z}_l \cos \zeta_l = 0$$

In our WMR the two wheels have a common axis and are unsteered. Therefore, $\zeta_r = \zeta_l = 0$. For WMRs with steered wheels we may have $\zeta_r \neq 0$, $\zeta_l \neq 0$. In our case $\cos \zeta_r = \cos \zeta_l = 1$, and so the two kinematic equations, solved for the angular wheel velocities $\dot{\theta}_r$ and $\dot{\theta}_l$, give:

$$\dot{\mathbf{q}} = \mathbf{J}^\dagger \dot{\mathbf{p}}, \quad \dot{\mathbf{q}} = \begin{bmatrix} \dot{\theta}_r \\ \dot{\theta}_l \end{bmatrix}$$

where the inverse Jacobian is:

$$\mathbf{J}^\dagger = \frac{1}{r} \begin{bmatrix} \cos \phi & \sin \phi & a & 1 & 0 & 0 & 0 \\ \cos \phi & \sin \phi & -a & 0 & 1 & 0 & 0 \end{bmatrix}$$

The nonholonomic constraints are written in Pfaffian form:

$$\mathbf{M}(\mathbf{p})\dot{\mathbf{p}} = \mathbf{0}$$

where

$$\mathbf{M}(\mathbf{p}) = \begin{bmatrix} -\sin \phi & \cos \phi & b & 0 & 0 & -1 & 0 \\ -\sin \phi & \cos \phi & b & 0 & 0 & 0 & -1 \end{bmatrix}$$

$$\dot{\mathbf{p}} = (\dot{x}_G, \dot{y}_G, \dot{\phi} \quad \vdots \quad \dot{w}_r, \dot{w}_l, \dot{z}_r, \dot{z}_l)^T$$

In the special case where only lateral slip takes place (i.e., $\dot{w}_r = 0$, $\dot{w}_l = 0$), the components \dot{w}_r and \dot{w}_l are dropped from $\dot{\mathbf{p}}$, and the matrices \mathbf{J}^\dagger and $\mathbf{M}(\mathbf{p})$ are reduced appropriately, having only five columns. Note that here the wheels are fixed and so $\dot{z}_r = \dot{z}_l = \dot{y}_r$ where \dot{y}_r is the lateral slipping velocity of the body of the WMR. Typically, the slipping variables, which are unknown and nonmeasurable are treated as disturbances via disturbance rejection and robust control techniques.

2.3.3 Tricycle

The motion of this WMR is controlled by the wheel steering angular velocity ω_ψ and its linear velocity v_w (or its angular velocity $\omega_w = \dot{\theta}_w = v_w/r$, where r is the radius of the wheel) (Figure 2.8).

The orientation angle and angular velocity are ϕ and $\dot{\phi}$, respectively. It is assumed that the vehicle has its guidance point Q in the back of the powered wheel (i.e., it has a central back axis). The state of the robot's motion is:

$$\mathbf{p} = [x_Q, y_Q, \phi, \psi]^T$$

The kinematic variables are:

Steering wheel velocity: $v_w = r\dot{\theta}_w$.

Vehicle velocity: $v = v_w \cos \psi = r(\cos \psi)\dot{\theta}_w$

Vehicle orientation velocity: $\dot{\phi} = (1/D)v_w \sin \psi$

Steering angle velocity: $\dot{\psi} = \omega_\psi$

Using the above relations we find:

$$\dot{\mathbf{p}} = \begin{bmatrix} \dot{x}_Q \\ \dot{y}_Q \\ \dot{\phi} \\ \dot{\psi} \end{bmatrix} = \begin{bmatrix} v \cos \phi \\ v \sin \phi \\ \dot{\phi} \\ \dot{\psi} \end{bmatrix} = \begin{bmatrix} r \cos \psi \cos \phi \\ r \cos \psi \sin \phi \\ (r/D) \sin \psi \\ 0 \end{bmatrix} \dot{\theta}_w + \begin{bmatrix} 0 \\ 0 \\ 0 \\ 1 \end{bmatrix} \dot{\psi} = \mathbf{J}\dot{\boldsymbol{\theta}} \quad (2.45)$$

where $\dot{\boldsymbol{\theta}} = [\dot{\theta}_w, \dot{\psi}]^T$ is the vector of joint velocities (control variables), and

$$\mathbf{J} = \begin{bmatrix} r \cos \psi \cos \phi & 0 \\ r \cos \psi \sin \phi & 0 \\ (r/D) \sin \psi & 0 \\ 0 & 1 \end{bmatrix} \quad (2.46)$$

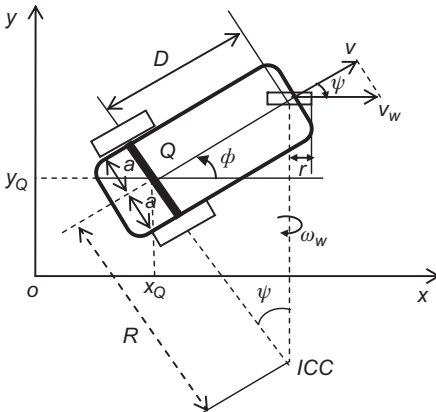


Figure 2.8 Geometry of the tricycle WMR (ψ is the steering angle).

is the Jacobian matrix. This Jacobian is again noninvertible, but we can find the inverse kinematic equations directly using the relations:

$$\dot{\phi}/v = (1/D)\tan\psi \text{ or } \psi = \arctan(D\dot{\phi}/v) \quad (2.47a)$$

and

$$\dot{\theta}_w = \frac{v_w}{r} = \frac{1}{r} \sqrt{v^2 + (D\dot{\phi})^2} \quad (2.47b)$$

The instantaneous curvature radius R is given by (Figure 2.8):

$$R = D \tan(\pi/2 - \psi(t)) \quad (2.48)$$

From Eq. (2.45) we see that the tricycle is again a 2-input driftless affine system with vector fields:

$$\mathbf{g}_1 = \begin{bmatrix} r \cos \psi \cos \phi \\ r \cos \psi \sin \phi \\ (r/D) \sin \psi \\ 0 \end{bmatrix}, \quad \mathbf{g}_2 = \begin{bmatrix} 0 \\ 0 \\ 0 \\ 1 \end{bmatrix}$$

that allow steering wheel motion $\dot{\theta}_w$, and steering angle motion $\dot{\psi}$, respectively.

2.3.4 Car-Like WMR

The geometry of the car-like mobile robot is shown in Figure 2.9A and the A.W.E. S.O.M.-9000 line-tracking car-like robot prototype (Aalborg University) in Figure 2.9B.

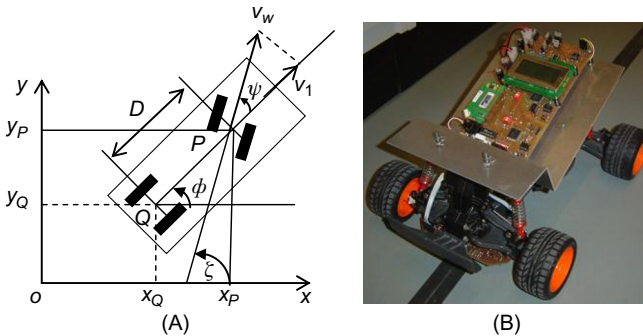


Figure 2.9 (A) Kinematic structure of a car-like robot, (B) A car-like robot prototype.

Source: <http://sqr-1.dk/robot/robot.php>

The state of the robot's motion is represented by the vector [20]:

$$\mathbf{p} = [x_Q, y_Q, \phi, \psi]^T \quad (2.49)$$

where x_Q, y_Q are the Cartesian coordinates of the wheel axis midpoint Q , ϕ is the orientation angle of the vehicle, and ψ is the steering angle. Here, we have two nonholonomic constraints, one for each wheel pair, that is:

$$-\dot{x}_Q \sin \phi + \dot{y}_Q \cos \phi = 0 \quad (2.50a)$$

$$-\dot{x}_p \sin(\phi + \psi) + \dot{y}_p \cos(\phi + \psi) = 0 \quad (2.50b)$$

where x_p and y_p are the position coordinates of the front wheels midpoint P . From Figure 2.9 we get:

$$x_p = x_Q + D \cos \phi, \quad y_p = y_Q + D \sin \phi$$

Using these relations the second kinematic constraint (2.50b) becomes:

$$-\dot{x}_Q \sin(\phi + \psi) + \dot{y}_Q \cos(\phi + \psi) + D(\cos \psi)\dot{\phi}$$

The two nonholonomic constraints are written in the matrix form:

$$\mathbf{M}(\mathbf{p})\dot{\mathbf{p}} = \mathbf{0} \quad (2.51a)$$

where

$$\mathbf{M}(\mathbf{p}) = \begin{bmatrix} -\sin \phi & \cos \phi & 0 & 0 \\ -\sin(\phi + \psi) & \cos(\phi + \psi) & D \cos \psi & 0 \end{bmatrix} \quad (2.51b)$$

The kinematic equations for a rear-wheel driving car are found to be (Figure 2.9):

$$\begin{aligned} \dot{x}_Q &= v_1 \cos \phi \\ \dot{y}_Q &= v_1 \sin \phi \\ \dot{\phi} &= \frac{1}{D} v_w \sin \psi \\ &= \frac{1}{D} v_1 \tan \psi \\ \dot{\psi} &= v_2 \end{aligned} \quad (2.52)$$

These equations can be written in the affine form:

$$\begin{bmatrix} \dot{x}_Q \\ \dot{y}_Q \\ \dot{\phi} \\ \dot{\psi} \end{bmatrix} = \begin{bmatrix} \cos \phi \\ \sin \phi \\ (1/D)tg\psi \\ 0 \end{bmatrix} v_1 + \begin{bmatrix} 0 \\ 0 \\ 0 \\ 1 \end{bmatrix} v_2 \quad (2.53)$$

that has the vector fields:

$$\mathbf{g}_1 = \begin{bmatrix} \cos \phi \\ \sin \phi \\ (1/D)tg\psi \\ 0 \end{bmatrix}, \quad \mathbf{g}_2 = \begin{bmatrix} 0 \\ 0 \\ 0 \\ 1 \end{bmatrix}$$

allowing the driving motion v_1 and the steering motion $v_2 = \dot{\psi}$, respectively. The Jacobian form of Eq. (2.53) is:

$$\dot{\mathbf{p}} = \mathbf{J}\mathbf{v}, \quad \mathbf{v} = [v_1, v_2]^T \quad (2.54)$$

with Jacobian matrix:

$$\mathbf{J} = \begin{bmatrix} \cos \phi & 0 \\ \sin \phi & 0 \\ (tg\psi)/D & 0 \\ 0 & 1 \end{bmatrix} \quad (2.55)$$

Here, there is a singularity at $\psi = \pm \pi/2$, which corresponds to the “jamming” of the WMR when the front wheels are normal to the longitudinal axis of its body. Actually, this singularity does not occur in practice due to the restricted range of the steering angle ψ ($-\pi/2 < \psi < \pi/2$).

The kinematic model for the front wheel driving vehicle is (Eqs. 2.45 and 2.46) [20]:

$$\dot{\mathbf{p}} = \mathbf{J}\mathbf{v}, \quad \mathbf{J} = \begin{bmatrix} \cos \phi \cos \psi & 0 \\ \sin \phi \cos \psi & 0 \\ (\sin \psi)/D & 0 \\ 0 & 1 \end{bmatrix} \quad (2.56a)$$

In this case the previous singularity does not occur, since at $\psi = \pm \pi/2$ the car can still (in principle) pivot about its rear wheels. Using the new inputs u_1 and u_2 defined as:

$$u_1 = v_1, u_2 = (1/D)\sin(\zeta - \phi)v_1 + v_2$$

the above model is transformed to:

$$\begin{bmatrix} \dot{x}_p \\ \dot{y}_p \\ \dot{\phi} \\ \dot{\zeta} \end{bmatrix} = \begin{bmatrix} \cos \zeta \\ \sin \zeta \\ (1/D)\sin(\zeta - \phi) \\ 0 \end{bmatrix} u_1 + \begin{bmatrix} 0 \\ 0 \\ 0 \\ 1 \end{bmatrix} u_2 \quad (2.56b)$$

where $\zeta = \phi + \psi$ is the total steering angle with respect to the axis Ox .

Indeed, from $x_p = x_Q + D \cos \phi$ and $y_p = y_Q + D \sin \phi$ (Figure 2.9), and Eq. (2.56a) we get:

$$\begin{aligned} \dot{x}_p &= \dot{x}_Q - D(\sin \phi)\dot{\phi} = (\cos \phi \cos \psi - \sin \phi \sin \psi)v_1 \\ &= [\cos(\phi + \psi)]v_1 = (\cos \zeta)u_1 \end{aligned}$$

$$\begin{aligned} \dot{y}_p &= \dot{y}_Q + D(\cos \phi)\dot{\phi} = (\sin \phi \cos \psi + \cos \phi \sin \psi)v_1 \\ &= [\sin(\phi + \psi)]v_1 = (\sin \zeta)u_1 \end{aligned}$$

$$\dot{\phi} = \frac{1}{D}[\sin(\zeta - \phi)]v_1 = \left[\frac{1}{D}\sin(\zeta - \phi) \right] u_1$$

$$\dot{\zeta} = \dot{\phi} + \dot{\psi} = \left[\frac{1}{D}\sin(\zeta - \phi) \right] v_1 + v_2 = u_2$$

We observe, from Eq. (2.56b), that the kinematic model for x_p , y_p , and ζ (i.e., the first, second, and fourth equation in Eq. (2.56b)) is actually a unicycle model (2.28a).

Two special cases of the above car-like model are known as:

- Reeds-Shepp car
- Dubins car

The *Reeds-Shepp car* is obtained by restricting the values of the velocity v_1 to three distinct values $+1$, 0 , and -1 . These values appear to correspond to three distinct “gears”: “forward,” “park,” or “reverse.” The *Dubins car* is obtained when the reverse motion is not allowed in the Reeds-Shepp car, that is, the value $v_1 = -1$ is excluded, in which case $v_1 = \{0, 1\}$.

Example 2.3

It is desired to find the steering angle ψ which is required for a rear-wheel driven car-like WMR to go from its present position $Q(x_Q, y_Q)$ to a given goal $F(x_f, y_f)$. The available data, which are obtained via proper sensors, are the distance L between (x_f, y_f) and (x_Q, y_Q) and the angle ε of the vector \vec{QF} with respect to the current vehicle orientation.

Solution

We will work with the geometry of Figure 2.10 [19]. The kinematic equations of the WMR are given by Eq. (2.52). The WMR will go from the position Q to the goal F following a circular path with curvature:

$$\frac{1}{R_1} = \frac{1}{D} \tan \psi$$

determined using the bicycle equivalent model, that combines the two front wheels and the two rear wheels (Figure 2.10, left).

On the other hand, the curvature $1/R_2$ of the circular path that passes through the goal, is obtained from the relation (Figure 2.10, right):

$$L/2 = R_2 \sin(\varepsilon)$$

that is:

$$\frac{1}{R_2} = \frac{2}{L} \sin(\varepsilon) \quad (2.57a)$$

To meet the goal tracking requirement the above two curvatures $1/R_1$ and $1/R_2$ must be the same, that is:

$$\frac{1}{D} \tan \psi = \frac{2}{L} \sin(\varepsilon)$$

Therefore:

$$\psi = \tan^{-1} \left(\frac{2D}{L} \sin(\varepsilon) \right) \quad (2.57b)$$

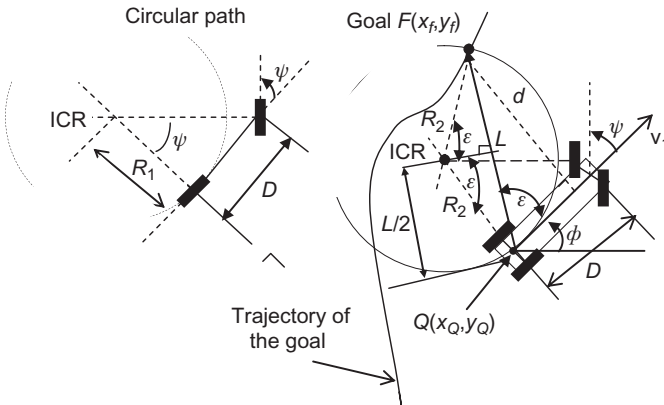


Figure 2.10 Geometry of the goal tracking problem.

Equation (2.57b) gives the steering angle ψ in terms of the data L and ε , and can be used to pursuit tracking of goals (targets) that are moving along given trajectories. In these cases the goal F lies at the intersection of the goal trajectory and the look-ahead circle. To get a better interpretation of (2.57a), we use the lateral distance d between the vehicles orientation (heading) vector and the goal point, which is given by (Figure 2.10):

$$d = L \sin(\varepsilon)$$

Then, the curvature $1/R_2$ in Eq. (2.57a) is given by:

$$\frac{1}{R_2} = \frac{2d}{L^2}$$

This indicates that the curvature $1/R_1$ of the path resulting from the steering angle ψ should be:

$$\frac{1}{R_1} = \left(\frac{2}{L^2}\right)d \quad (2.57c)$$

Equation (2.57c) is a “proportional control law” and shows that the curvature $1/R_1$ of the robot’s path should be proportional to the cross track error d some look-ahead distance in front of the WMR with a gain $2/L^2$.

2.3.5 Chain and Brockett—Integrator Models

The general 2-input n -dimensional chain model (briefly $(2, n)$ -chain model) is:

$$\begin{aligned} \dot{x}_1 &= u_1 \\ \dot{x}_2 &= u_2 \\ \dot{x}_3 &= x_2 u_1 \\ &\vdots \\ \dot{x}_n &= x_{n-1} u_1 \end{aligned} \quad (2.58)$$

The *Brockett* (single) *integrator* model is:

$$\begin{aligned} \dot{x}_1 &= u_1 \\ \dot{x}_2 &= u_2 \\ \dot{x}_3 &= x_1 u_2 - x_2 u_1 \end{aligned} \quad (2.59)$$

and the *double integrator* model is:

$$\begin{aligned} \dot{x}_1 &= u_1 \\ \dot{x}_2 &= u_2 \\ \dot{x}_3 &= x_1 \dot{x}_2 - x_2 \dot{x}_1 \end{aligned} \quad (2.60)$$

The nonholonomic WMR kinematic models can be transformed to the above models. Here, the unicycle model (which also covers the differential drive model) and the car-like model will be considered.

2.3.5.1 Unicycle WMR

The unicycle kinematic model is given by Eq. (2.26):

$$\dot{x}_Q = v_Q \cos \phi, \quad \dot{y}_Q = v_Q \sin \phi, \quad \dot{\phi} = v_\phi \quad (2.61)$$

Using the transformation:

$$\begin{aligned} z_1 &= \phi \\ z_2 &= x_Q \cos \phi + y_Q \sin \phi \\ z_3 &= x_Q \sin \phi - y_Q \cos \phi \end{aligned} \quad (2.62)$$

the unicycle model is converted to the (2,3)-chain form:

$$\begin{aligned} \dot{z}_1 &= u_1 \\ \dot{z}_2 &= u_2 \\ \dot{z}_3 &= z_2 u_1 \end{aligned} \quad (2.63)$$

where $u_1 = v_\phi$ and $u_2 = v_Q - z_3 u_1$.

Defining new state variables:

$$x_1 = z_1, \quad x_2 = z_2, \quad x_3 = -2z_3 + z_1 z_2 \quad (2.64)$$

the (2,3)-chain model is converted to the *Brockett integrator*:

$$\begin{aligned} \dot{x}_1 &= u_1 \\ \dot{x}_2 &= u_2 \\ \dot{x}_3 &= x_1 u_2 - x_2 u_1 \end{aligned} \quad (2.65)$$

2.3.5.2 Rear-Wheel Driving Car

The rear-wheel driven car model is given by Eq. (2.52):

$$\dot{x}_Q = v_1 \cos \phi, \quad \dot{y}_Q = v_1 \sin \phi, \quad \dot{\phi} = \frac{v_1}{D} \operatorname{tg} \psi, \quad \dot{\psi} = v_2 \quad (2.66)$$

Using the state transformation:

$$x_1 = x_Q, \quad x_2 = \frac{\operatorname{tg} \psi}{D \cos^3 \phi}, \quad x_3 = \operatorname{tg} \phi, \quad x_4 = y_Q \quad (2.67)$$

and input transformation:

$$v_1 = u_1 / \cos \phi \quad (2.68)$$

$$v_2 = -\frac{3 \sin^2 \psi \sin \phi}{D \cos^2 \phi} u_1 + D \cos^2 \psi (\cos^3 \phi) u_2$$

for $\phi \neq \pi/2 \pm k\pi$ and $\psi \neq \pi/2 \pm k\pi$, the model (2.66) is converted to the (2,4)-chain form:

$$\begin{aligned} \dot{x}_1 &= u_1 \\ \dot{x}_2 &= u_2 \\ \dot{x}_3 &= x_2 u_1 \\ \dot{x}_4 &= x_3 u_1 \end{aligned} \quad (2.69)$$

2.3.6 Car-Pulling Trailer WMR

This is an extension of the car-like WMR, where N one-axis trailers are attached to a car-like robot with rear-wheel drive. This type of trailer is used, for example, at airports for transporting luggage. The form of equations depend crucially on the exact point at which the trailer is attached and on the choice of body frames. Here, for simplicity each trailer will be assumed to be connected to the axle midpoint of the previous trailer (*zero hooking*) as shown in Figure 2.11 [20].

The new parameter introduced here is the distance from the center of the back axle of trailer i to the point at which is hitched to the next body. This is called the *hitch* (or *hinge-to-hinge*) length denoted by L_i . The car length is D . Let ϕ_i be

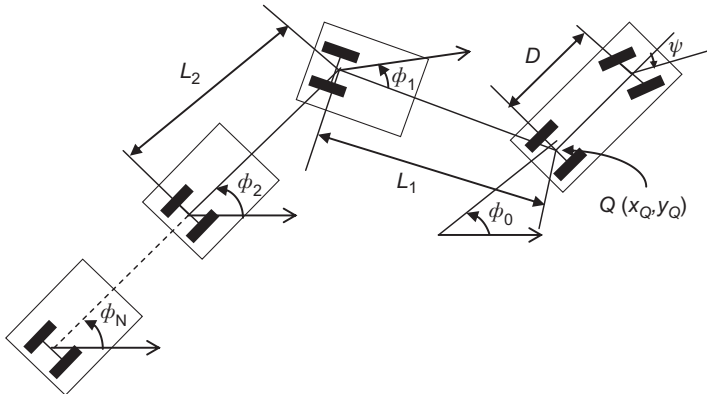


Figure 2.11 Geometrical structure of the N -trailer WMR.

the orientation of the i th trailer, expressed with respect to the world coordinate frame. Then from the geometry of Figure 2.11 we get the following equations:

$$\begin{aligned} x_i &= x_Q - \sum_{j=1}^i L_j \cos \phi_j \\ y_i &= y_Q - \sum_{j=1}^i L_j \sin \phi_j \end{aligned} \quad i = 1, 2, \dots, N$$

which give the following nonholonomic constraints:

$$\begin{aligned} \dot{x}_Q \sin \phi_0 - \dot{y}_Q \cos \phi_0 &= 0 \\ \dot{x}_Q \sin(\phi_0 + \psi) - \dot{y}_Q \cos(\phi_0 + \psi) - \dot{\phi}_0 D \cos \psi &= 0 \\ \dot{x}_Q \sin \phi_i - \dot{y}_Q \cos \phi_i + \sum_{j=1}^i \dot{\phi}_j L_j \cos(\phi_i - \phi_j) &= 0 \end{aligned}$$

for $i = 1, 2, \dots, N$.

In analogy to Eq. (2.52) the kinematic equations of the N -trailer are found to be:

$$\begin{aligned} \dot{x}_Q &= v_1 \cos \phi_0 \\ \dot{y}_Q &= v_1 \sin \phi_0 \\ \dot{\phi}_0 &= (1/D)v_1 \tan \psi \\ \dot{\psi} &= v_2 \\ \dot{\phi}_1 &= \frac{1}{L_1} \sin(\phi_0 - \phi_1) \\ \dot{\phi}_2 &= \frac{1}{L_2} \cos(\phi_0 - \phi_1) \sin(\phi_1 - \phi_2) \\ &\vdots \\ \dot{\phi}_i &= \frac{1}{L_i} \prod_{j=1}^{i-1} \cos(\phi_{j-1} - \phi_j) \sin(\phi_{i-1} - \phi_i) \\ &\vdots \\ \dot{\phi}_N &= \frac{1}{L_N} \prod_{j=1}^{N-1} \cos(\phi_{j-1} - \phi_j) \sin(\phi_{N-1} - \phi_N) \end{aligned} \tag{2.70}$$

which, obviously, represent a driftless affine system with two inputs $u_1 = v_1$ and $u_2 = v_2$ and $N + 4$, states:

$$\dot{\mathbf{x}} = \mathbf{g}_1(\mathbf{x})u_1 + \mathbf{g}_2(\mathbf{x})u_2$$

We observe that the first four lines of the fields \mathbf{g}_1 and \mathbf{g}_2 represent the (powered) car-like WMR itself.

2.4 Omnidirectional WMR Kinematic Modeling

The following WMRs will be considered [2,4,11,12,16]:

- Multiwheel omnidirectional WMR with orthogonal (universal) wheels
- Four-wheel omnidirectional WMR with mecanum wheels that have a roller angle $\pm 45^\circ$.

2.4.1 Universal Multiwheel Omnidirectional WMR

The geometric structure of a multiwheel omnirobot is shown in Figure 2.12A. Each wheel has three velocity components [16]:

- Its own velocity $v_i = r\dot{\theta}_i$, where r is the common wheel radius and $\dot{\theta}_i$ its own angular velocity
- An induced velocity $v_{i,\text{roller}}$ which is due to the free rollers (here assumed of the universal type; roller angle $\pm 90^\circ$)
- A velocity component v_ϕ which is due to the rotation of the robotic platform about its center of gravity Q , that is, $v_\phi = D\dot{\phi}$, where $\dot{\phi}$ is the angular velocity of the platform and D is the distance of the wheel from Q .

Here, the roller angle is $\pm 90^\circ$, and so:

$$v_h^2 = v_i^2 + v_{i,\text{roller}}^2 \quad (2.71a)$$

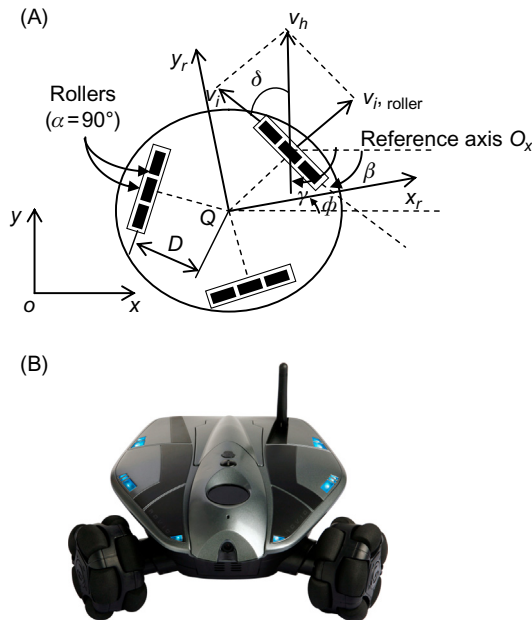


Figure 2.12 (A) Velocity vector of wheel i . The velocity v_h is the robot vehicle velocity due to the wheel motion, (B) An example of a 3-wheel setup.

Source: <http://deviceguru.com/files/rovio-3.jpg>.

where

$$\begin{aligned}
 v_i &= v_h \cos(\delta) \\
 &= v_h \cos(\gamma - \beta) \\
 &= v_h(\cos \gamma \cos \beta + \sin \gamma \sin \beta)
 \end{aligned} \tag{2.71b}$$

Thus the total velocity of the wheel i is:

$$\begin{aligned}
 v_i &= v_h(\cos \gamma \cos \beta + \sin \gamma \sin \beta) + D\dot{\phi} \\
 &= v_{hx} \cos \beta + v_{hy} \sin \beta + D\dot{\phi}
 \end{aligned} \tag{2.72}$$

where v_{hx} and v_{hy} are the x, y components of v_h , that is:

$$v_{hx} = v_h \cos \gamma, \quad v_{hy} = v_h \sin \gamma$$

Equation (2.72) is general and can be used in WMRs with any number of wheels.

Thus, for example, in the case of a 3-wheel robot we may choose the angle β for the wheels 1, 2, and 3 as 0° , 120° , and 240° , respectively, and get the equations:

$$v_1 = v_{hx} + D\dot{\phi}, \quad v_2 = -\frac{1}{2}v_{hx} + \frac{\sqrt{3}}{2}v_{hy} + D\dot{\phi}, \quad v_3 = -\frac{1}{2}v_{hx} - \frac{\sqrt{3}}{2}v_{hy} + D\dot{\phi} \tag{2.73}$$

with $v_i = r\dot{\theta}_i$. Now, defining the vectors:

$$\dot{\mathbf{p}}_h = [v_{hx}, v_{hy}, \dot{\phi}]^T, \quad \dot{\mathbf{q}} = [\dot{\theta}_1, \dot{\theta}_2, \dot{\theta}_3]^T$$

we can write Eq. (2.73) in the inverse Jacobian form:

$$\dot{\mathbf{q}} = \mathbf{J}^{-1} \dot{\mathbf{p}}_h \tag{2.74a}$$

where

$$\mathbf{J}^{-1} = \frac{1}{r} \begin{bmatrix} 1 & 0 & D \\ -1/2 & \sqrt{3}/2 & D \\ -1/2 & -\sqrt{3}/2 & D \end{bmatrix} \tag{2.74b}$$

Here $\det \mathbf{J} \neq 0$, and Eq. (2.74a) can be inverted to give $\dot{\mathbf{p}}_h = \mathbf{J}\dot{\mathbf{q}}$.

It is remarked that using omniwheels at different angles we can obtain an overall velocity of the WMR's platform which is greater than the maximum angular

velocity of each wheel. For example, selecting in the above 3-wheel case $\beta = 60^\circ$ and $\gamma = 90^\circ$ we get from Eq. (2.71b):

$$v_i = \frac{\sqrt{3}}{2} v_h, \text{ i.e., } v_h = \frac{2}{\sqrt{3}} v_i > v_i$$

The ratio v_h/v_i is called the *velocity augmentation factor* (VAF) [16]:

$$\text{VAF} = v_h/v_i$$

and depends on the number of wheels used and their angular positions on the robot's body. As a further example, consider a 4-wheel robot with $\beta = 45^\circ$ and $\gamma = 90^\circ$. Then, Eq. (2.71b) gives:

$$\text{VAF} = \sqrt{2}$$

Example 2.4

We are given the 4-universal-wheel omnidirectional robot of Figure 2.13, where the angles of the wheels with respect to the axis Qx_r of the vehicle's coordinate frame are β_i ($i = 1, 2, 3, 4$). Derive the kinematic equations of the robot in terms of the unit directional vectors \mathbf{u}_i ($i = 1, 2, 3, 4$) of the wheel velocities, with respect to the local coordinate frame $Qx_r y_r$.

Solution

Let $\dot{\phi}$ be the robot's angular velocity, and \mathbf{v}_Q its linear velocity with world-frame coordinates \dot{x}_Q and \dot{y}_Q .

The unit directional vectors of the wheel velocities are:

$$\mathbf{u}_1 = \begin{bmatrix} -\sin \beta_1 \\ \cos \beta_1 \end{bmatrix}, \quad \mathbf{u}_2 = \begin{bmatrix} -\sin \beta_2 \\ \cos \beta_2 \end{bmatrix}, \quad \mathbf{u}_3 = \begin{bmatrix} -\sin \beta_3 \\ \cos \beta_3 \end{bmatrix}, \quad \mathbf{u}_4 = \begin{bmatrix} 0 \\ 1 \end{bmatrix}$$

where it was assumed that the axis of wheel 4 coincides with axis Qx_r .

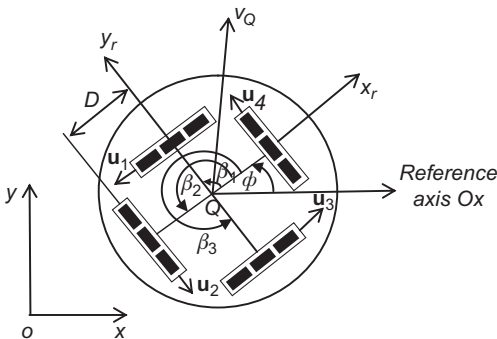


Figure 2.13 Four-wheel omnidirectional robot.

The relation between \dot{x}_Q , \dot{y}_Q and \dot{x}_r , \dot{y}_r is given by the rotational matrix $\mathbf{R}(\phi)$ (Eq. 2.17), that is:

$$\begin{bmatrix} \dot{x}_Q \\ \dot{y}_Q \end{bmatrix} = \begin{bmatrix} \cos \phi & -\sin \phi \\ \sin \phi & \cos \phi \end{bmatrix} \begin{bmatrix} \dot{x}_r \\ \dot{y}_r \end{bmatrix} = \mathbf{R}(\phi) \begin{bmatrix} \dot{x}_r \\ \dot{y}_r \end{bmatrix}$$

or

$$\begin{bmatrix} \dot{x}_r \\ \dot{y}_r \end{bmatrix} = \begin{bmatrix} \cos \phi & \sin \phi \\ -\sin \phi & \cos \phi \end{bmatrix} \begin{bmatrix} \dot{x}_Q \\ \dot{y}_Q \end{bmatrix} = \mathbf{R}^{-1}(\phi) \begin{bmatrix} \dot{x}_Q \\ \dot{y}_Q \end{bmatrix}$$

Now, we have:

$$\begin{aligned} v_1 = r\dot{\theta}_1 &= \mathbf{u}_1^T \begin{bmatrix} \dot{x}_r \\ \dot{y}_r \end{bmatrix} + D\dot{\phi} = \mathbf{u}_1^T \mathbf{R}^{-1}(\phi) \begin{bmatrix} \dot{x}_Q \\ \dot{y}_Q \end{bmatrix} + D\dot{\phi} \\ v_2 = r\dot{\theta}_2 &= \mathbf{u}_2^T \begin{bmatrix} \dot{x}_r \\ \dot{y}_r \end{bmatrix} + D\dot{\phi} = \mathbf{u}_2^T \mathbf{R}^{-1}(\phi) \begin{bmatrix} \dot{x}_Q \\ \dot{y}_Q \end{bmatrix} + D\dot{\phi} \\ v_3 = r\dot{\theta}_3 &= \mathbf{u}_3^T \begin{bmatrix} \dot{x}_r \\ \dot{y}_r \end{bmatrix} + D\dot{\phi} = \mathbf{u}_3^T \mathbf{R}^{-1}(\phi) \begin{bmatrix} \dot{x}_Q \\ \dot{y}_Q \end{bmatrix} + D\dot{\phi} \\ v_4 = r\dot{\theta}_4 &= \mathbf{u}_4^T \begin{bmatrix} \dot{x}_r \\ \dot{y}_r \end{bmatrix} + D\dot{\phi} = \mathbf{u}_4^T \mathbf{R}^{-1}(\phi) \begin{bmatrix} \dot{x}_Q \\ \dot{y}_Q \end{bmatrix} + D\dot{\phi} \end{aligned}$$

or, in compact, form:

$$\dot{\mathbf{q}} = \mathbf{J}^{-1} \dot{\mathbf{p}}_Q \quad (2.75a)$$

where

$$\dot{\mathbf{q}} = \begin{bmatrix} \dot{\theta}_1 \\ \dot{\theta}_2 \\ \dot{\theta}_3 \\ \dot{\theta}_4 \end{bmatrix}, \quad \dot{\mathbf{p}}_Q = \begin{bmatrix} \dot{x}_Q \\ \dot{y}_Q \\ \dot{\phi} \end{bmatrix} \quad (2.75b)$$

$$\mathbf{J}^{-1} = \frac{1}{r} (\mathbf{U}^T \mathbf{R}^{-1}(\phi) + \bar{\mathbf{D}}) \quad (2.75c)$$

with:

$$\mathbf{U} = [\mathbf{u}_1 \quad \vdots \quad \mathbf{u}_2 \quad \vdots \quad \mathbf{u}_3 \quad \vdots \quad \mathbf{u}_4], \quad \bar{\mathbf{D}} = [D, \quad D, \quad D, \quad D]^T \quad (2.75d)$$

As usual, this inverse Jacobian equation gives the required angular wheel speeds $\dot{\theta}_i (i = 1, 2, 3, 4)$ that lead to the desired linear velocity $[\dot{x}_Q, \dot{y}_Q]$, and angular velocity $\dot{\phi}$ of the robot. A discussion of the modeling and control problem of a WMR with this structure is provided in Ref. [17].

2.4.2 Four–Wheel Omnidirectional WMR with Mecanum Wheels

Consider the 4-wheel WMR of Figure 2.14, where the mecanum wheels have roller angle $\pm 45^\circ$ [2,4].

Here, we have four-wheel coordinate frames $O_{ci}(i = 1, 2, 3, 4)$. The angular velocity \dot{q}_i of the wheel i has three components:

1. $\dot{\theta}_{ix}$: rotation speed around the hub
2. $\dot{\theta}_{ir}$: rotation speed of the roller i
3. $\dot{\theta}_{iz}$: rotation speed of the wheel around the contact point.

The wheel velocity vector $\mathbf{v}_{ci} = [\dot{x}_{ci}, \dot{y}_{ci}, \dot{\phi}_{ci}]^T$ in O_{ci} coordinates is given by:

$$\begin{bmatrix} \dot{x}_{ci} \\ \dot{y}_{ci} \\ \dot{\phi}_{ci} \end{bmatrix} = \begin{bmatrix} 0 & r_i \sin \alpha_i & 0 \\ R_i & -r_i \cos \alpha_i & 0 \\ 0 & 0 & 1 \end{bmatrix} \begin{bmatrix} \dot{\theta}_{ix} \\ \dot{\theta}_{ir} \\ \dot{\theta}_{iz} \end{bmatrix} \quad (2.76)$$

for $i = 1, 2, 3, 4$, where R_i is the wheel radius, r_i is the roller radius, and α_i the roller angle. The robot velocity vector $\dot{\mathbf{p}}_Q = [\dot{x}_Q, \dot{y}_Q, \dot{\phi}_Q]^T$ in the Ox_Qy_Q coordinate frame (Eqs. 2.9–2.13) is:

$$\dot{\mathbf{p}}_Q = \begin{bmatrix} \dot{x}_Q \\ \dot{y}_Q \\ \dot{\phi}_Q \end{bmatrix} = \begin{bmatrix} \cos \phi_{ci}^Q & -\sin \phi_{ci}^Q & d_{ciy}^Q \\ \sin \phi_{ci}^Q & \cos \phi_{ci}^Q & -d_{cix}^Q \\ 0 & 0 & 1 \end{bmatrix} \begin{bmatrix} \dot{x}_{ci} \\ \dot{y}_{ci} \\ \dot{\phi}_{ci} \end{bmatrix} \quad (2.77)$$

where ϕ_{ci}^Q denotes the rotation angle (orientation) of the frame O_{ci} with respect to Qx_Qy_Q , and d_{cix}^Q, d_{ciy}^Q are the translations of O_{ci} with respect to Qx_Qy_Q . Introducing Eq. (2.76) into Eq. (2.77) we get:

$$\dot{\mathbf{p}}_Q = \mathbf{J}_i \dot{\mathbf{q}}_i \quad (i = 1, 2, 3, 4) \quad (2.78)$$

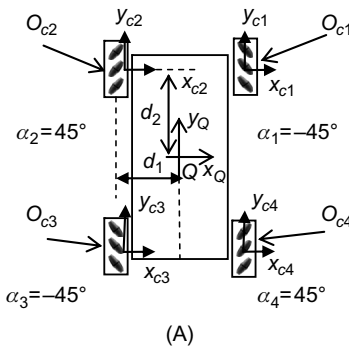


Figure 2.14 Four-mecanum-wheel WMR (A) Kinematic geometry (B) A real 4-mecanum-wheel WMR.

Source: <http://www.automotto.com/entry/airtrax-wheels-go-in-any-direction>.

where $\dot{\mathbf{q}}_i = [\dot{\theta}_{ix}, \dot{\theta}_{ir}, \dot{\theta}_{iz}]^T$, and

$$\mathbf{J}_i = \begin{bmatrix} -R_i \sin \phi_{ci}^Q & r_i \sin(\phi_{ci}^Q + \alpha_i) & d_{ciy}^Q \\ R_i \cos \phi_{ci}^Q & -r_i \cos(\phi_{ci}^Q + \alpha_i) & -d_{cix}^Q \\ 0 & 0 & 1 \end{bmatrix} \quad (2.79)$$

is the Jacobian matrix of wheel i , which is square and invertible. If all wheels are identical (except for the orientation of the rollers), the kinematic parameters of the robot in the configuration shown in Figure 2.14 are:

$$\begin{aligned} R_i &= R, \quad r_i = r, \quad \phi_{ci}^Q = 0 \\ |d_{cix}^Q| &= d_1, \quad |d_{ciy}^Q| = d_2 \\ \alpha_1 &= \alpha_3 = -45^\circ, \quad \alpha_2 = \alpha_4 = 45^\circ \end{aligned} \quad (2.80)$$

Thus, the Jacobian matrices (2.79) are:

$$\begin{aligned} \mathbf{J}_1 &= \begin{bmatrix} 0 & -r\sqrt{2}/2 & d_2 \\ R & -r\sqrt{2}/2 & d_1 \\ 0 & 0 & 1 \end{bmatrix}, \quad \mathbf{J}_2 = \begin{bmatrix} 0 & r\sqrt{2}/2 & d_2 \\ R & -r\sqrt{2}/2 & -d_1 \\ 0 & 0 & 1 \end{bmatrix} \\ \mathbf{J}_3 &= \begin{bmatrix} 0 & -r\sqrt{2}/2 & -d_2 \\ R & -r\sqrt{2}/2 & -d_1 \\ 0 & 0 & 1 \end{bmatrix}, \quad \mathbf{J}_4 = \begin{bmatrix} 0 & r\sqrt{2}/2 & -d_2 \\ R & -r\sqrt{2}/2 & d_1 \\ 0 & 0 & 1 \end{bmatrix} \end{aligned} \quad (2.81)$$

The robot motion is produced by the simultaneous motion of all wheels.

In terms of $\dot{\theta}_{ix}$ (i.e., the wheels' angular velocities around their axles) the velocity vector $\dot{\mathbf{p}}_Q$ is given by:

$$\begin{bmatrix} \dot{x}_Q \\ \dot{y}_Q \\ \dot{\phi}_Q \end{bmatrix} = \frac{R}{4} \begin{bmatrix} \frac{-1}{d_1 + d_2} & \frac{1}{d_1 + d_2} & \frac{-1}{d_1 + d_2} & \frac{1}{d_1 + d_2} \\ \frac{1}{d_1 + d_2} & \frac{1}{d_1 + d_2} & \frac{1}{d_1 + d_2} & \frac{1}{d_1 + d_2} \\ \frac{1}{d_1 + d_2} & \frac{-1}{d_1 + d_2} & \frac{-1}{d_1 + d_2} & \frac{1}{d_1 + d_2} \end{bmatrix} \begin{bmatrix} \dot{\theta}_{1x} \\ \dot{\theta}_{2x} \\ \dot{\theta}_{3x} \\ \dot{\theta}_{4x} \end{bmatrix} \quad (2.82)$$

The robot speed vector $\dot{\mathbf{p}} = [\dot{x}, \dot{y}, \dot{\phi}]^T$ in the world coordinate frame is obtained as:

$$\begin{bmatrix} \dot{x} \\ \dot{y} \\ \dot{\phi} \end{bmatrix} = \begin{bmatrix} \cos \phi & -\sin \phi & 0 \\ \sin \phi & \cos \phi & 0 \\ 0 & 0 & 1 \end{bmatrix} \begin{bmatrix} \dot{x}_Q \\ \dot{y}_Q \\ \dot{\phi}_Q \end{bmatrix} \quad (2.83)$$

where ϕ is the rotation angle of the platform's coordinate frame Qx_Qy_Q around the z axis which is orthogonal to Oxy . Inverting Eqs. (2.82) and (2.83) we get the

inverse kinematic model, which gives the angular speeds $\dot{\theta}_{ix} (i = 1, 2, 3, 4)$ of the wheels around their hubs required to get a desired speed $[\dot{x}, \dot{y}, \dot{\phi}]^T$ of the robot:

$$\begin{bmatrix} \dot{\theta}_{1x} \\ \dot{\theta}_{2x} \\ \dot{\theta}_{3x} \\ \dot{\theta}_{4x} \end{bmatrix} = \frac{1}{R} \begin{bmatrix} -1 & 1 & (d_1 + d_2) \\ 1 & 1 & -(d_1 + d_2) \\ -1 & 1 & -(d_1 + d_2) \\ 1 & 1 & (d_1 + d_2) \end{bmatrix} \begin{bmatrix} \dot{x}_Q \\ \dot{y}_Q \\ \dot{\phi}_Q \end{bmatrix} \quad (2.84)$$

$$\begin{bmatrix} \dot{x}_Q \\ \dot{y}_Q \\ \dot{\phi}_Q \end{bmatrix} = \begin{bmatrix} \cos \phi & \sin \phi & 0 \\ -\sin \phi & \cos \phi & 0 \\ 0 & 0 & 1 \end{bmatrix} \begin{bmatrix} \dot{x} \\ \dot{y} \\ \dot{\phi} \end{bmatrix} \quad (2.85)$$

For historical awareness, we mention here that the mecanum wheel was invented by the Swedish engineer *Bengt Ilon* in 1973 during his work at the Swedish company Mecanum AB. For this reason it is also known as *Ilon wheel* or *Swedish wheel*.

Example 2.5

It is desired to construct a mecanum wheel with n rollers of angle α . Determine the roller length D_r and the thickness d of the wheel.

Solution

We consider the wheel geometry shown in Figure 2.15, where R is the wheel radius [18].

From this figure we get the following relations:

$$n = 2\pi / \phi \quad (2.86a)$$

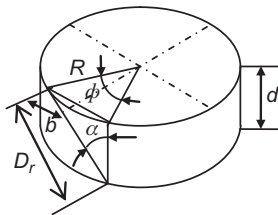
$$\sin(\phi/2) = b/R \quad (2.86b)$$

$$2b = D_r \sin \alpha \quad (2.86c)$$

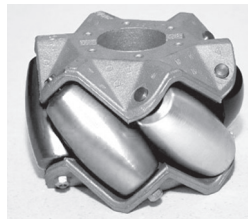
$$d = D_r \cos \alpha \quad (2.86d)$$

From Eq. (2.86a–c) we have:

$$\sin\left(\frac{\pi}{n}\right) = \left(\frac{D_r}{2R}\right) \sin \alpha \quad (2.87)$$



(A)



(B)

Figure 2.15 (A) Geometry of mecanum wheel where the rollers are assumed to be placed peripherally, (B) A 6-roller wheel example.

Source: <http://store.kornylak.com/SearchResults.asp?Cat=7>.

whence:

$$D_r = 2R \frac{\sin(\pi/n)}{\sin\alpha} \quad (2.88)$$

Solving (2.87) for $\sin\alpha$ and noting that $\cos\alpha = \sin\alpha/\tan\alpha$, (2.86d) gives:

$$d = 2R \frac{\sin(\pi/n)}{\tan\alpha} \quad (2.89)$$

For a roller angle $\alpha = 45^\circ$, Eqs. (2.88) and (2.89) give:

$$D_r = 2\sqrt{2}R \sin(\pi/n) \quad (2.90a)$$

$$d = 2R \sin(\pi/n) \quad (2.90b)$$

For a roller angle $\alpha = 90^\circ$ (universal wheel) we get:

$$D_r = 2R \sin(\pi/n) \quad (2.91a)$$

$$d = 0 \quad (\text{ideally}) \quad (2.91b)$$

In this case, d can have any convenient value required by other design considerations.

References

- [1] Angelo A. Robotics: a reference guide to new technology. Boston, MA: Greenwood Press; 2007.
- [2] Muir PF, Neuman CP. Kinematic modeling of wheeled mobile robots. J Rob Syst 1987;4(2):281–329.
- [3] Alexander JC, Maddocks JH. On the kinematics of wheeled mobile robots. Int J Rob Res 1981;8(5):15–27.
- [4] Muir PF, Neuman C. Kinematic modeling for feedback control of an omnidirectional wheeled mobile robot. In: Proceedings of IEEE international conference on robotics and automation, Raleigh, NC; 1987, p. 1772–8.
- [5] Kim DS, Hyun Kwon W, Park HS. Geometric kinematics and applications of a mobile robot. Int J Control Autom Syst 2003;1(3):376–84.
- [6] Rajagopalan R. A generic kinematic formulation for wheeled mobile robots. J Rob Syst 1997;14:77–91.
- [7] Sreenivasan SV. Kinematic geometry of wheeled vehicle systems. In: Proceedings of 24th ASME mechanism conference, Irvine, CA, 96-DETC-MECH-1137; 1996.
- [8] Balakrishna R, Ghosal A. Two dimensional wheeled vehicle kinematics. IEEE Trans Rob Autom 1995;11(1):126–30.
- [9] Killough SM, Pin FG. Design of an omnidirectional and holonomic wheeled platform design. In: Proceedings of IEEE conference on robotics and automation, Nice, France; 1992, p. 84–90.

- [10] Sidek N, Sarkar N. Dynamic modeling and control of nonholonomic mobile robot with lateral slip. In: Proceedings of seventh WSEAS international conference on signal processing robotics and automation (ISPRA'08), Cambridge, UK; February 20–22, 2008, p. 66–74.
- [11] Giovanni I. Swedish wheeled omnidirectional mobile robots: kinematics analysis and control. *IEEE Trans Rob* 2009;25(1):164–71.
- [12] West M, Asada H. Design of a holonomic omnidirectional vehicle. In: Proceedings of IEEE conference on robotics and automation, Nice, France; May 1992, p. 97–103.
- [13] Chakraborty N, Ghosal A. Kinematics of wheeled mobile robots on uneven terrain. *Mech Mach Theory* 2004;39:1273–87.
- [14] Sordalen OJ, Egeland O. Exponential stabilization of nonholonomic chained systems. *IEEE Trans Autom Control* 1995;40(1):35–49.
- [15] Khalil H. *Nonlinear Systems*. Upper Saddle River, NJ: Prentice Hall; 2001.
- [16] Ashmore M, Barnes N. Omni-drive robot motion on curved paths: the fastest path between two points is not a straight line. In: Proceedings of 15th Australian joint conference on artificial intelligence: advances in artificial intelligence (AI'02). London: Springer; 2002. p. 225–36.
- [17] Huang L, Lim YS, Li D, Teoh CEL. Design and analysis of a four-wheel omnidirectional mobile robot. In: Proceedings of second international conference on autonomous robots and agents, Palmerston North, New Zealand; December 2004. p. 425–8.
- [18] Doroftei I, Grosu V, Spinu V. Omnidirectional mobile robot: design and implementation. In: Habib MK, editor. *Bioinspiration and robotics: walking and climbing robots*. Vienna, Austria: I-Tech; 2007. p. 512–27.
- [19] Phairoh T, Williamson K. Autonomous mobile robots using real time kinematic signal correction and global positioning system control. In: Proceedings of 2008 IAJC-IJME international conference on engineering and technology, Sheraton, Nashville, TN; November 2008, Paper 087/IT304.
- [20] De Luca A, Oriolo G, Samson C. Feedback control of a nonholonomic car-like robot. In: Laumond J-P, editor. *Robot motion planning and control*. Berlin, New York: Springer; 1998. p. 171–253.